Atmos. Meas. Tech., 9, 2135–2145, 2016
www.atmos-meas-tech.net/9/2135/2016/
doi:10.5194/amt-9-2135-2016

Atmospheric Measurement Techniques Open Access EGU

Detection of dimethylamine in the low pptv range using nitrate chemical ionization atmospheric pressure interface time-of-flight (CI-APi-TOF) mass spectrometry

Mario Simon[1], Martin Heinritzi[1], Stephan Herzog[1], Markus Leiminger[1], Federico Bianchi[2,3], Arnaud Praplan[4], Josef Dommen[2], Joachim Curtius[1], and Andreas Kürten[1]

[1]Institute for Atmospheric and Environmental Sciences, Goethe University of Frankfurt, 60438 Frankfurt am Main, Germany
[2]Laboratory of Atmospheric Chemistry, Paul-Scherrer-Institute, 5232 Villigen, Switzerland
[3]Institute for Atmospheric and Climate Science, ETH Zürich, 8092 Zürich, Switzerland
[4]Helsinki Institute of Physics, University of Helsinki, 00014 Helsinki, Finland

Correspondence to: Mario Simon (simon@iau.uni-frankfurt.de)

Received: 30 September 2015 – Published in Atmos. Meas. Tech. Discuss.: 17 December 2015
Revised: 15 April 2016 – Accepted: 18 April 2016 – Published: 13 May 2016

Abstract. Amines are potentially important for atmospheric new particle formation, but their concentrations are usually low with typical mixing ratios in the pptv range or even smaller. Therefore, the demand for highly sensitive gas-phase amine measurements has emerged in the last several years. Nitrate chemical ionization mass spectrometry (CIMS) is routinely used for the measurement of gas-phase sulfuric acid in the sub-pptv range. Furthermore, extremely low volatile organic compounds (ELVOCs) can be detected with a nitrate CIMS. In this study we demonstrate that a nitrate CIMS can also be used for the sensitive measurement of dimethylamine (DMA, $(CH_3)_2NH$) using the $NO_3^- \cdot (HNO_3)_{1-2} \cdot$(DMA) cluster ion signal. Calibration measurements were made at the CLOUD chamber during two different measurement campaigns. Good linearity between 0 and ∼ 120 pptv of DMA as well as a sub-pptv detection limit of 0.7 pptv for a 10 min integration time are demonstrated at 278 K and 38 % RH.

1 Introduction

Amines are potentially an important agent contributing to atmospheric aerosol nucleation events in those regions where amines are emitted. Their measurement in the gas phase has therefore recently received considerable attention. A large variety of different amines exists in the atmosphere and various sources of amines are known, such as animal husbandry or sewage; nevertheless, the gas-phase concentrations of amines are expected to be low due to rapid uptake into acidic aerosol and high solubility (Ge et al., 2011a, b). Despite concentrations expected to be typically 10 to 1000 times below atmospheric gas-phase ammonia levels, amines such as methyl-, dimethyl-, or trimethylamine were postulated to enhance the nucleation of sulfuric acid much more efficiently than NH_3 (Kurtén et al., 2008). Furthermore, it was found that typical concentration levels of H_2SO_4 and NH_3 in the boundary layer are too low to explain aerosol formation rates as frequently observed during nucleation events via nucleation mechanisms such as binary H_2SO_4-H_2O or NH_3-ternary nucleation (Kirkby et al., 2011).

Participation of amines in nucleation was studied in the laboratory for the amine–sulfuric acid–water system (e.g., Berndt et al., 2010; Erupe et al., 2011; Zollner et al., 2012; Almeida et al., 2013; Berndt et al., 2014; Kürten et al., 2014; Bianchi et al., 2014; Jen et al., 2015; Glasoe et al., 2015). Almeida et al. (2013) showed for dimethylamine (DMA, $(CH_3)_2NH$) that the presence of a few pptv enhances the aerosol formation rates of sulfuric acid by several orders of magnitude, and formation rates that are typical for atmospheric nucleation events are observed. Kürten et al. (2014) and Jen et al. (2014) studied the formation of neutral (i.e.,

uncharged) H_2SO_4–DMA clusters and showed that the cluster formation process proceeds at or near the kinetic limit (Rao and McMurry, 1989) when the DMA to sulfuric acid ratio is high ($\sim$ 10 to 100). This means that for the low abundances of H_2SO_4 and DMA (H_2SO_4 at sub-pptv level, DMA at pptv level) the growth is limited only by the arrival rate of H_2SO_4 molecules and an efficient acid–base stabilization prevents even the smallest H_2SO_4–DMA clusters (i.e., the sulfuric acid dimer) from evaporation.

Evidence for the participation of amines in aerosol nucleation in the boundary layer has been found (e.g., Mäkelä et al., 2001; Smith et al., 2010; Zhao et al., 2011; Creamean et al., 2011; Yu et al., 2012; Chen et al., 2012). However, the extent to which amines are participating in atmospheric nucleation is still not established. This is to a large degree due to the difficulty of measuring amines in real time at low pptv to sub-pptv mixing ratios. Mass spectrometric methods using a chemical ionization mass spectrometer (CIMS) have become available for amine measurements. These methods have sufficient time resolution and high sensitivity to measure atmospherically relevant mixing ratios in a range between $\sim$ 0.1 and 40 pptv. Various amines were detected by positive-ion chemical ionization via ambient pressure proton transfer (Hanson et al., 2011; Freshour et al., 2014). Protonated ethanol or acetone ions were used as reagent ions by Yu and Lee (2012). Negative-ion detection of amines using bisulfate reagent ions has been described recently (Sipilä et al., 2015).

Here we describe the detection of gas-phase DMA at sub-pptv levels at the Cosmics Leaving OUtdoor Droplets Chamber (CLOUD) aerosol chamber at CERN by use of a nitrate chemical ionization atmospheric pressure interface time-of-flight mass spectrometer (CI-APi-TOF-MS; Jokinen et al., 2012; Kürten et al., 2014). Nitrate chemical ionization mass spectrometry is used frequently for the highly sensitive detection of H_2SO_4 (Tanner and Eisele, 1991; Kürten et al., 2011) and also for the detection of extremely low volatile organic compounds (ELVOCs; Ehn et al., 2014). The fact that DMA can be measured in the presence of H_2SO_4 and ELVOCs is very useful as all three compounds are relevant for aerosol nucleation and growth. The method and the detection scheme are described in detail; absolute concentrations are derived by calculating the DMA mixing ratios from the balance of sources and sinks in the CLOUD chamber. DMA detection limits are discussed. Furthermore, the method is also compared with DMA measurements by ion chromatography (Praplan et al., 2012).

2 Methods

2.1 CLOUD facility

The CLOUD chamber at CERN is a 26 m^3 cylindrical vessel that is used to study aerosol processes such as new particle formation. The inner surfaces consist of electropolished stainless steel. Great effort is made to minimize contamination by any condensable substances that may influence new particle formation. The chamber and its components have been described in detail before (Kirkby et al., 2011; Kupc et al., 2011; Voigtländer et al., 2012). For this study results are reported from the CLOUD7 and CLOUD10-T experiments (October–December 2012 and April–May 2015) in which the aerosol nucleation for the sulfuric acid–water–dimethylamine system was investigated (Almeida et al., 2013; Kürten et al., 2014). All measurements were carried out at a temperature of 278 K and a relative humidity of 38 % in the chamber.

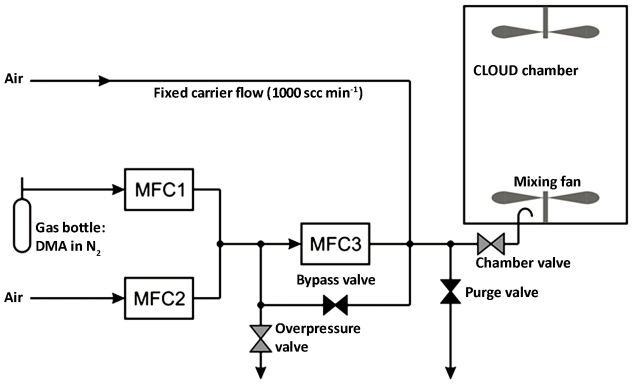

Figure 1. CLOUD chamber and gas system for delivering DMA to the chamber. Three mass flow controllers (MFC1 to MFC3) and several valves are used to control the flow rates. The figure indicates a setting where the bypass and the purge valve are closed while the other valves are open.

2.2 Gas system and calculated DMA mixing ratios

A schematic drawing of the gas system and the CLOUD chamber is shown in Fig. 1. A specially designed gas system has been implemented at CLOUD for precisely controlling the amount of dimethylamine which is fed into the chamber. The gas system for each individual trace gas includes three calibrated mass flow controllers (MFCs) and several valves for diluting a mixture from a gas bottle with clean air before it is fed into the chamber close to the lower mixing fan.

The amount of DMA introduced into the chamber can be calculated from the fraction B of DMA inside the gas bottle ($B = 0.01$) and the MFC flow rates (see Fig. 1). When the bypass valve is closed, which was the case at all times during CLOUD7 and CLOUD10-T, the following amount of DMA enters the chamber:

$$A_{\mathrm{DMA}} = \frac{\mathrm{MFC1} \cdot \mathrm{MFC3}}{\mathrm{MFC1} + \mathrm{MFC2}} \cdot B. \quad (1)$$

The flow rates (denoted with MFC1, MFC2, and MFC3) have units of $cm^3\ s^{-1}$ (at standard temperature and pressure – STP – in this case 293.15 K and 1013 hPa), and the quantity A_{DMA}

is the flow rate of DMA. The volume mixing ratio (VMR) of DMA (in pptv) inside the CLOUD chamber can be derived from the following differential equation:

$$\frac{\mathrm{d}\,\mathrm{VMR_{DMA}}}{\mathrm{d}t} = \frac{A_{\mathrm{DMA}}}{V_{\mathrm{ch}}} \cdot 10^{12}\mathrm{pptv} - k_{\mathrm{wall}} \cdot \mathrm{VMR_{DMA}} - k_{\mathrm{dil}} \cdot \mathrm{VMR_{DMA}}. \quad (2)$$

Here, V_{ch} is the chamber volume (2.61×10^7 cm^3, where V_{ch} denotes a physical volume), k_{wall} is the wall loss rate constant for DMA, and k_{dil} is the dilution rate constant. The dilution rate constant can be calculated from the ratio of the clean gas flow rate that is required to replenish the gas taken by the instruments and the chamber volume. In this study, the flow rate of air into the chamber is 160 L min^{-1} at standard temperature and pressure, which yields a dilution rate constant (assuming homogenous mixing) of 1×10^{-4} s^{-1}. Assuming that the walls act as a perfect sink the wall loss rate can be assumed to be proportional to the square root of the gas-phase diffusion coefficient for an aerosol chamber (Crump and Seinfeld, 1981). For sulfuric acid the wall loss rate constant was experimentally determined as 2.2×10^{-3} s^{-1}. For DMA it should be higher because it is a lighter molecule compared to sulfuric acid and has a higher diffusivity. The value for sulfuric acid therefore provides a lower limit for the wall loss rate of DMA.

Assuming steady state in Eq. (2) yields

$$\mathrm{VMR_{DMA}} = \frac{A_{\mathrm{DMA}} \cdot 10^{12}\mathrm{pptv}}{V_{\mathrm{ch}} \cdot (k_{\mathrm{wall}} + k_{\mathrm{dil}})} = \frac{\mathrm{MFC1} \cdot \mathrm{MFC3}}{\mathrm{MFC1} + \mathrm{MFC2}} \cdot \frac{B \cdot 10^{12}\mathrm{pptv}}{V_{\mathrm{ch}} \cdot (k_{\mathrm{wall}} + k_{\mathrm{dil}})} = \frac{F}{k_{\mathrm{wall}} + k_{\mathrm{dil}}}. \quad (3)$$

The factor F describes the addition of DMA to the chamber in units of pptv s^{-1}. The unknown quantity k_{wall} could in principle be derived from Eq. (3) by calibration experiments if a reference instrument for the measurement of DMA were used. Alternatively, the wall loss rate can be determined from the decay rate of the signal, which is used to calculate the DMA mixing ratio in this study (see Sect. 3.1).

It should be noted that the effect of DMA condensation on aerosol particles, which are formed during nucleation experiments, is not taken into account in Eqs. (2) and (3). For the data shown in this study, either no sulfuric acid was generated when the DMA calibration measurements (see Sect. 3.2) were performed or the sulfuric acid and the associated condensation sink was so low that it had no effect on the DMA mixing ratio.

The assumption that the DMA mixing ratio is at equilibrium inside the pipes once the chamber valve is opened, i.e., that wall loss is negligible for the DMA inlet lines, is justified due to the following reasons. First, the gas lines are conditioned over a duration of at least 24 h before DMA is added to the chamber for the first time. During this time the purge valve is open and the chamber valve is closed (Fig. 1). Only the last ∼ 23 cm between the chamber valve and the point where the DMA enters the chamber are therefore not conditioned. Second, the mixing ratio of DMA inside the gas lines is generally higher than several tens of ppbv even though the DMA inside the chamber is in the pptv range due to the strong dilution inside the chamber. The high DMA mixing ratio enables a rapid equilibration of the short unconditioned section of the gas lines.

2.3 CI-APi-TOF instrument

The CI-APi-TOF mass spectrometer has been described previously (Jokinen et al., 2012; Kürten et al., 2014). The CI-APi-TOF combines an atmospheric pressure chemical ionization source based on the design by Eisele and coworkers (Eisele and Tanner, 1993) and a high-resolution atmospheric pressure interface time-of-flight mass spectrometer (Tofwerk AG, Switzerland). The ion source uses a corona discharge for the primary ion generation (Kürten et al., 2011). Nitrate ions ($NO_3^- \bullet (HNO_3)_x$) are generally used for the detection of sulfuric acid and sulfuric acid–amine clusters but more recently it was found that they also allow for the detection of ELVOCs (see, e.g., Ehn et al., 2014). Owing to the high mass resolving power (∼ 4500 Th Th^{-1}) and the high mass accuracy (better than 10 ppm) of the CI-APi-TOF these ions can be unambiguously identified in this study if additional information like the isotopic pattern is taken into account. These features will minimize potential interferences especially in field measurements, where a lot of unknown compounds are potentially present.

One important aspect to consider is sampling line losses when evaluating the DMA signals. During CLOUD10-T the CI-APi-TOF was connected to the chamber by its own sampling line, while in CLOUD7 the instrument was sharing the sampling line with another instrument. Therefore, a y-splitter was used. For this kind of inlet the sampling line losses cannot be easily calculated in the same way as for a straight tube and laminar flow. Instead, the effective length method (Karlsson and Martinsson, 2003) was used after comparing the sulfuric acid concentrations measured by a CIMS and the CI-APi-TOF simultaneously. Since the CIMS was connected to the CLOUD chamber with its own dedicated sampling line, the loss rate could be quantified for sulfuric acid. Taking into account the independently determined calibration constant regarding sulfuric acid for the CIMS and the CI-APi-TOF (Kürten et al., 2012, 2014) an effective length of ∼ 1.5 m could be determined for the CI-APi-TOF sampling line at a flow rate of 8.5 L min^{-1} (at STP) for sulfuric acid. These values are used in the next section for deriving the transmission efficiency of DMA to the CI-APi-TOF.

2.4 Ionization process

In contrast to the detection of gaseous sulfuric acid (H_2SO_4) by a proton transfer reaction which leads to the formation

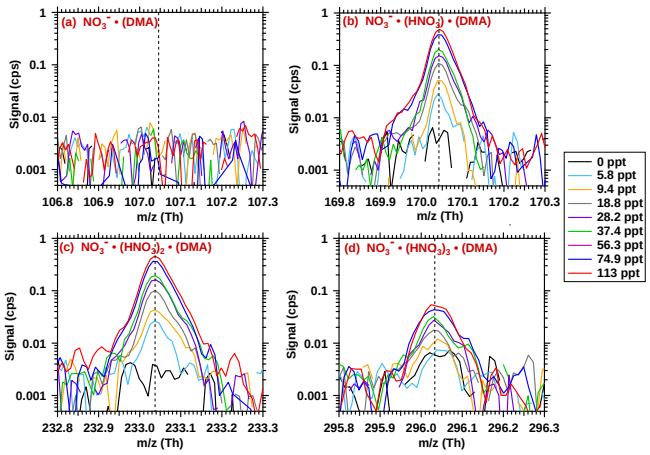

Figure 2. High-resolution mass spectra for narrow ranges of m/z values corresponding to $NO_3^-\cdot(HNO_3)_{0-3}\cdot(DMA)$ ions. Compared to the DMA ion signals the nitrate primary ion count rates were $\sim$13 500 cps (for NO_3^-), $\sim$2600 cps (for $NO_3^-\cdot(HNO_3)$), and $\sim$340 cps (for $NO_3^-\cdot(HNO_3)_2$). The colors indicate different mixing ratios that were established in the CLOUD chamber during calibration measurements and the dashed vertical lines show the exact mass of the cluster ions.

of bisulfate ions (HSO_4^-, Eisele and Tanner, 1993), dimethylamine is detected due to its ability to cluster with the $NO_3^-\cdot(HNO_3)_{x=1-3}$ primary ions:

$$\mathrm{DMA} + NO_3^-\cdot(HNO_3) \rightarrow NO_3^-\cdot(HNO_3)\cdot(\mathrm{DMA}) \quad (R1)$$

$$\mathrm{DMA} + NO_3^-\cdot(HNO_3)_{\geq 2} \rightarrow NO_3^-\cdot(HNO_3)_{\geq 2}\cdot(\mathrm{DMA}). \quad (R2)$$

The association Reactions (R1) and (R2) could both occur in the ion–molecule reaction zone ($\sim$50 ms reaction time) of the CI-APi-TOF; however, DMA is mainly detected at integer mass m/z 170 Th ($NO_3^-\cdot(HNO_3)\cdot$(DMA) ions) and integer mass m/z 233 Th ($NO_3^-\cdot(HNO_3)_2\cdot$(DMA)) (Fig. 2c and c). In addition, a small signal at m/z 296 Th ($NO_3^-\cdot(HNO_3)_3\cdot$(DMA)) is also visible in the mass spectra at high DMA mixing ratios (Fig. 2d). Since fragmentation could occur in the APi section, it is possible that this fragmentation is responsible for a high signal at m/z 170 Th although Reaction (R2) could be dominant. Regarding the identification and quantification of the mentioned signals it should be noted that even though integer masses are mentioned, the CI-APi-TOF mass spectra are evaluated using high-resolution data. The data are processed using tofTools developed by the University of Helsinki (Junninen et al., 2010).

To quantify the DMA concentration, the sum of the two most intense DMA signals is normalized by the primary ion count rate at m/z 188 Th ($NO_3^-\cdot(HNO_3)_2$). Tentatively, we have chosen the $NO_3^-\cdot(HNO_3)_2$ ion as the reference because it seems likely that this produces more stable cluster ions compared to $NO_3^-\cdot(HNO_3)$ due to an efficient acid–base stabilization mechanism (1 : 1 ratio between acid and base if the NO_3^- is regarded as a Lewis base). In previous CLOUD studies a similar scheme has been observed for ion clusters involving sulfuric acid and ammonia or dimethylamine (see Kirkby et al., 2011; Almeida et al., 2013; Kürten et al., 2014; Bianchi et al., 2014). Furthermore, Ortega et al. (2014) reported that a cluster of two acid molecules and one base molecule (e.g., $(H_2SO_4)_2\cdot$DMA) will only be stable in the neutral case. As soon as this cluster is negatively charged it becomes unstable and the base molecule will evaporate rapidly. In contrast, a cluster containing two acids besides the ion and a base molecule ($HSO_4^-\cdot(H_2SO_4)_2\cdot$DMA) will be much more stable. Although, the acid is in our case HNO_3 and not H_2SO_4 we believe that qualitatively the ion cluster chemistry for the two acids is similar. Future studies will show to what extent this assumption holds true. This leads to the following equation for the DMA concentration:

$$[\mathrm{DMA}] = C \cdot \mathrm{SL} \cdot \ln\left(1 + \frac{(\mathrm{CR}_{170} + \mathrm{CR}_{233})}{\mathrm{CR}_{188}}\right) \approx C \cdot \mathrm{SL} \cdot \frac{(\mathrm{CR}_{170} + \mathrm{CR}_{233})}{\mathrm{CR}_{188}}. \quad (4)$$

The factor C (in molecule cm^{-3}) can be derived from calibration measurements using the CLOUD chamber. Generally DMA mixing ratios are reported rather than concentrations and therefore the calibration factor has a different unit than in Eq. (4). However, the derived calibration constant can be converted to molecule cm^{-3} (see Sect. 3.2). An additional factor, SL (inverse of the penetration usually used to characterize sampling line losses of aerosol particles and molecules in tubes), is required to take into account losses of DMA molecules in the CI-APi-TOF sampling line during the transport from the chamber to the instrument; the parameters CR_{170}, CR_{233}, and CR_{188} denote the count rates at the exact masses for the $NO_3^-\cdot(HNO_3)_{1,2}\cdot$(DMA) and the $NO_3^-\cdot(HNO_3)_2$ ions, respectively. The factor SL has a value of $\sim$2.5 for CLOUD10-T. During CLOUD7 the factor has a value of $\sim$4 and was evaluated based on the effective length method mentioned in the previous section. For the evaluation of SL it was assumed that the diffusivity of H_2SO_4 at 278 K and 38 % relative humidity equals 0.07 cm^2 s^{-1} (Hanson and Eisele, 2000). For DMA a value of 0.10 cm^2 s^{-1} was assumed, which follows when scaling the reported value in Freshour et al. (2014) to the temperature of this study using a power dependency of 1.75 for the temperature dependence of the diffusion coefficient.

To our knowledge the existence of ion clusters containing amines and nitrate has been reported only once by Luts et al. (2011). They added diethylamine ($CH_3CH_2NHCH_2CH_3$, DEA) to ions created from ambient air and identified the cluster $NO_3^-\cdot(HNO_3)\cdot$(DEA) (m/z 198 Th). Additionally, signals at m/z 261 and m/z 334 Th were observed, which were tentatively assigned to the clusters $NO_3^-\cdot(HNO_3)_2\cdot$(DEA) and $NO_3^-\cdot(HNO_3)_2\cdot(\mathrm{DEA})_2$. This study is in agreement with the findings by Luts et al. (2011)

regarding the clusters containing one amine molecule; however, we did not observe a cluster containing two DMA molecules. Combining the results of the present study and the one by Luts et al. (2011) indicates that nitrate chemical ionization mass spectrometry should likely be capable of detecting various other amines and not just DMA or DEA.

Figure 2 shows high-resolution mass spectra for the m/z values corresponding to the $NO_3^- \cdot (HNO_3)_{0-3} \cdot (DMA)$ ions when different amounts of DMA were added to the CLOUD chamber (the indicated mixing ratios are discussed further below). Clearly it can be seen that the $NO_3^- \cdot (DMA)$ ion never exceeds the background level (Fig. 2a), indicating that this ion is very unstable and breaks up either in the ion drift tube or inside the CI-APi-TOF vacuum chamber. For the other signals the intensity increases with increasing DMA mixing ratio.

3 Results and discussion

3.1 DMA wall loss and dilution rate

The data shown in Fig. 3 were used experimentally to determine the wall loss rate of DMA in the CLOUD chamber during CLOUD7. The same procedure was repeated for CLOUD10-T. The red line shows the sum of the signals for $NO_3^- \cdot (HNO_3)_1 \cdot (DMA)$ and $NO_3^- \cdot (HNO_3)_2 \cdot (DMA)$ normalized by the count rate from the $NO_3^- \cdot (HNO_3)_2$ primary ion. Additionally, the setting of the DMA flow into the CLOUD chamber is shown in arbitrary units (shaded area in Fig. 3). When the DMA flow is shut off, a clear decrease in the DMA signal can be seen. This decay is due to two different loss processes: (1) wall loss, which is fast, and (2) mainly loss due to dilution, which is a slow process (see Sect. 2.2). However, this latter loss process is influenced by re-evaporation of DMA from the chamber walls. Fitting the decay with a double-exponential function yields a value for the wall loss rate of $2.3 \times 10^{-3}\,s^{-1}$. Comparison to the wall loss rate of sulfuric acid ($2.2 \times 10^{-3}\,s^{-1}$) confirms that the derived wall loss rate for DMA is reasonable. One expects a slightly higher loss rate for DMA because it is the lighter molecule and therefore diffuses faster. The fact that the wall loss rate for DMA is slightly faster than the one found for sulfuric acid implies that the walls act as a perfect sink for DMA under these experimental conditions (i.e., low DMA mixing ratios, short exposure time, 278 K, and 38 % RH). Furthermore, this assumption should be justified by the fact that the calibration lines (discussed in Sect. 3.2) show no steepening when going from low mixing ratios to higher values, which is evidence that no wall saturation occurs. However, when measuring higher mixing ratios over a long time it will probably be necessary either to clean the sampling line occasionally or to calibrate with a known amine concentration. The re-evaporation of DMA mentioned above therefore seems to have only a small effect and comes into play only when the flow of DMA into the chamber is shut off and the DMA concentration reaches very low values. The DMA wall loss rate of $2.8 \times 10^{-3}\,s^{-1}$ for CLOUD10-T is slightly higher due to a different configuration of the mixing fans inside the chamber resulting in a different thickness of the diffusion layer.

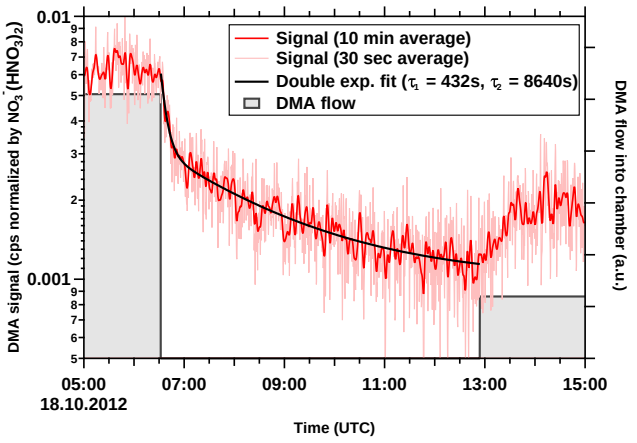

Figure 3. Decay of the normalized cluster ion signal indicating the DMA concentration with 10 min time resolution (red line) and 30 s time resolution (light red line). The DMA flow (grey line and area) into the chamber is shut off at ∼ 6:32 UTC and turned on again (at a lower set point) around 12:54 UTC. Using a double-exponential fit (black line) the decaying signal can be well represented. The first inverse decay constant represents the wall loss rate ($1/\tau_1 = 2.3 \times 10^{-3}\,s^{-1}$), while the second decay ($1/\tau_2 = 1.2 \times 10^{-4}\,s^{-1}$) represents a source term due to slow re-evaporation of DMA from the chamber walls superimposed by dilution.

Using the derived wall loss rate, the DMA mixing ratio can be calculated according to Eq. (3). The error in the targeted mixing ratio during CLOUD7 is calculated based on the 1σ standard deviations for the parameter τ_1 (τ_1 is the average decay time, i.e., the inverse of the wall loss rate, $\tau_1 = 432 \pm 48$ s) from the double-exponential fit which was made with the software IGOR. Furthermore, a 5 % error in the MFC flow rates is taken into account in the error analysis.

3.2 Sensitivity and linearity

Different flow rates of DMA were applied to the chamber during both CLOUD campaigns and for certain periods the DMA was completely shut off. The periods when the chamber was flushed with clean air for extended times, can be used to determine the background signal for the $NO_3^- \cdot (HNO_3)_{1-2} \cdot (DMA)$ cluster ions. We believe that this background is caused by electronic noise, since no DMA was detected in the clusters for the nucleation experiments conducted during these periods (Kürten et al., 2014). Since the CI-APi-TOF uses the same clean gas as the CLOUD chamber for the sheath gas it is also unlikely that there is any source of DMA inside the instrument.

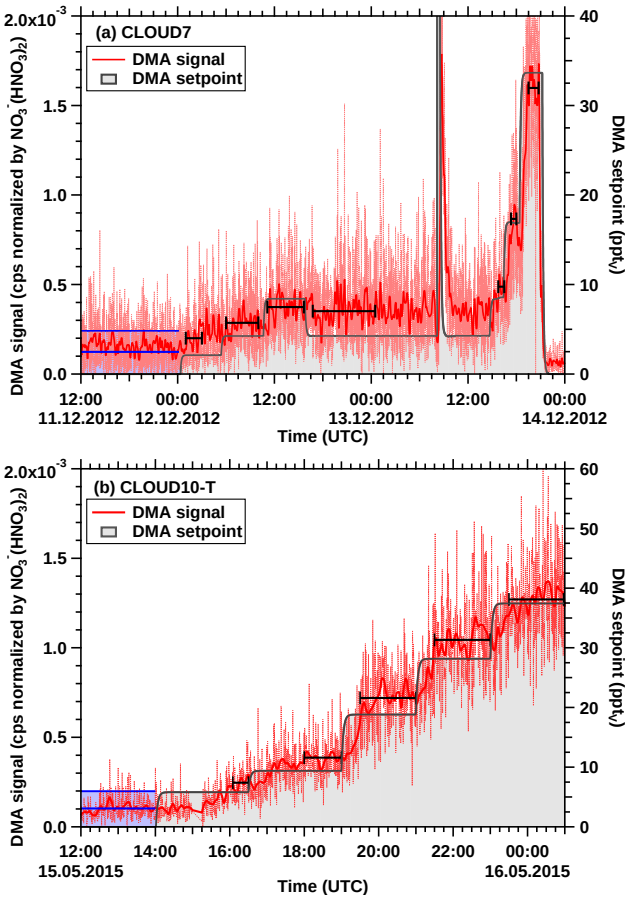

Figure 4. Time series of the normalized cluster ion signal indicating the DMA concentration with 10 min resolution (red lines) and 30 s time resolution (light red line) during the CLOUD7 **(a)** and CLOUD10-T **(b)** calibration. The grey lines and areas indicate the targeted DMA mixing ratios due to the MFC setting for the gas system. The average background signals including the 3σ standard deviation are shown by the horizontal blue lines and the light blue bands. The black lines illustrate the averaged periods. At the end of the displayed period in panel A the instrument was disconnected from the chamber and pure nitrogen was sampled; therefore the DMA signal drops immediately while DMA was still added in the chamber.

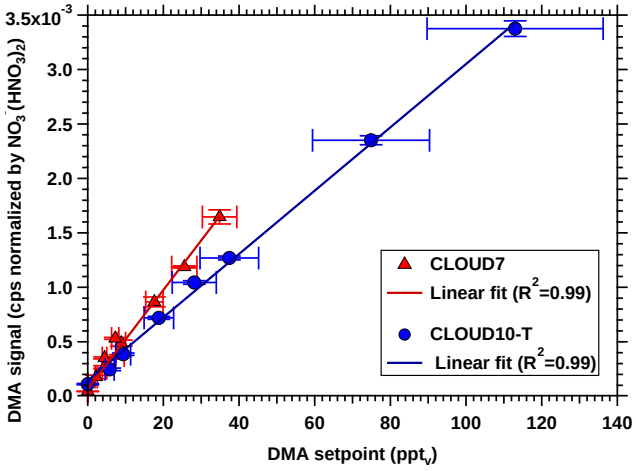

Figure 5. Calibration curves for the average DMA signals as a function of the DMA mixing ratio during CLOUD7 (red symbols) and CLOUD10-T (blue symbols). The linear fit for the CLOUD7 calibration follows the expression $y = 9.13 \times 10^{-5} + 4.41 \times 10^{-5}\,\mathrm{pptv}^{-1} \times x$. The expression for the linear fit of the CLOUD10-T (blue) calibration follows $y = 14.35 \times 10^{-5} + 2.91 \times 10^{-5}\,\mathrm{pptv}^{-1} \times x$. Error bars for the DMA set-point values are based on a ±5 % uncertainty for each of the MFC flow rate settings and the standard deviation of the fit parameter for k_{wall}. The errors for the measured DMA signals are based on the standard deviation of the mean.

Figure 4 shows the time series of the normalized DMA signal (red line) during CLOUD7 and CLOUD10-T together with the calculated DMA mixing ratio (shaded area) according to Eq. (2). It can be seen in Fig. 4a that even at the lowest set point of ∼ 2.2 pptv DMA the signal is significantly elevated compared to background conditions. Further increase of the DMA flow leads to correspondingly higher signals.

The data from Fig. 4 and from other periods (not shown) have been averaged over sufficiently long periods where a constant DMA mixing ratio was applied to the chamber. These averaged normalized signals are shown as a function of the calculated DMA mixing ratio in Fig. 5. A linear fit has been applied to the data from each calibration, yielding a correlation coefficient close to 1 ($R^2 = 0.99$). This indicates that the applied methodology is capable of quantifying DMA at low mixing ratios in the pptv range. However, note that for mixing ratios below 7 pptv additional effects of the CLOUD chamber itself, like re-evaporation of DMA from the chamber walls and conditioning of the DMA inlet lines, might enhance the equilibrium time significantly and therefore introduce additional uncertainty.

The slopes of the calibration line from Fig. 5 are a measure of the sensitivity of the nitrate CI-APi-TOF towards DMA. After converting the mixing ratio of DMA into a concentration (1 pptv corresponds to 2.61×10^7 molecule cm^{-3} at 278 K and 1 bar), the calibration constant from Eq. (4) can be evaluated as $C = 1.48 \times 10^{11}$ molecule cm^{-3} for CLOUD7 and $C = 3.45 \times 10^{11}$ molecule cm^{-3} for CLOUD10-T from the slope of the individual linear fit. Compared to the calibration constant for sulfuric acid this value is about 1 to 1.5 orders of magnitude higher (Kürten et al., 2012, 2014) and therefore indicates a lower sensitivity for DMA compared to sulfuric acid. One explanation for this behavior could be that the evaporation rate of the $NO_3^- \cdot (HNO_3)_{1-2} \cdot$(DMA) clusters regarding DMA is non-negligible. It is still an open question whether this evaporation occurs inside the ion source, where the temperature is close to the chamber temperature or within the APi section (first stage which is below ambient pressure), where a higher effective temperature is expected due to energetic collisions of the ions (that are accelerated by

electric fields) and neutral gas molecules. In order to avoid ambiguity due to changes in the primary ion count rate distribution over time, routinely performed calibration measurements are therefore recommended (Freshour et al., 2014). In this case, the method should yield accurate and reproducible results despite the yet unknown details of the ion–molecule clustering and declustering processes involved.

3.3 Limit of detection (LOD) for measurement of DMA

The data shown in Fig. 5 can be used to determine the LOD for the DMA measurements with the nitrate CI-APi-TOF. The average background signal together with the 3σ standard deviation is indicated by the light blue band in Fig. 4. The second step in Fig. 4a (4.4 pptv of DMA) during the CLOUD7 calibration yields an average signal that is outside the blue band. By use of the 3σ standard deviation the LOD during the CLOUD7 campaign was below 2.6 pptv for a 10 min integration time.

Since the CI-APi-TOF sampling line in CLOUD7 leads to a factor of 4 reduction in the DMA concentration reaching the instrument, a considerably lower detection limit (~ 0.7 pptv) would result for a situation where sampling line losses are negligible. While zero wall loss cannot be realized in reality, a considerable reduction in the sampling line losses can be achieved in field studies. The CLOUD sampling lines are relatively long (~ 1 m in total) and the instrument operated at a low flow rate ($\sim 8.5\,\mathrm{L\,min^{-1}}$). In the field there is no restriction on the available amount of air that can be drawn; therefore reduced line losses may be realized. During the CLOUD10-T calibration (Fig. 4b) the first step (5.8 pptv of DMA) is clearly above the LOD. This is supported by the determination of the LOD which was below 1.7 pptv for the CLOUD10-T campaign. Taking the sampling loss of a factor ~ 2.5 into account yields an LOD of ~ 0.7 pptv, which matches very well with the value obtained for CLOUD7.

3.4 Comparison to previously published DMA mixing ratios from CLOUD

One important aspect of the present study is that the DMA mixing ratios are calculated for the CLOUD chamber from the evaluated wall loss rate for DMA and the MFC settings. A comparison to DMA mixing ratios measured directly using an ion chromatograph (IC; see Praplan et al., 2012) yields generally reasonable agreement for the CLOUD7 data for the time periods when both instruments where operated in parallel with the settings reported here (Fig. 6). The DMA average mixing ratio (averaged for the time period displayed) was 17 pptv for the IC and 22 pptv for the CI-APi-TOF. During the CLOUD10-T measurements the IC was not available. Note that the displayed DMA mixing ratios from the IC for CLOUD7 have been multiplied by a factor of 1.8 to account for the efficiency of the cation trap column. This correction was not considered in previous publications and therefore

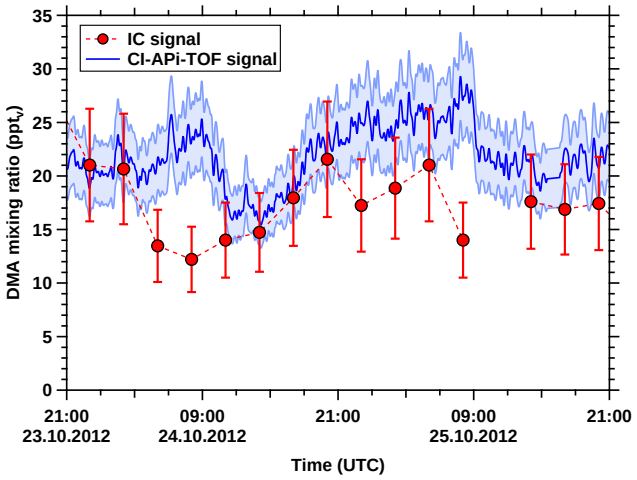

Figure 6. Comparison between the measured ion chromatograph (IC) signal and the calculated CI-APi-TOF signal in pptv. The CI-APi-TOF signal is determined by the raw ion counts multiplied by the calibration factor C, which is defined by the slope of the linear fit for CLOUD7 (red line of Fig. 4). Both signals show in general a reasonable agreement but the IC signal is lower on average and point-to-point variability is large. The uncertainty (shown as error bars) of the IC instrument ($\pm 25\,\%$) is based on the calibration. The 14 % uncertainty of the CI-APi-TOF is shown as light blue shaded area. The mean values over the entire time period displayed are 17 ± 3 pptv for the IC and 22 ± 3 pptv for the CI-APi-TOF.

some of the reported DMA mixing ratios should be scaled up by a factor of 1.8. Some of the high concentration points reported in Almeida et al. (2013) are from CLOUD7 and need to be scaled up, while the low concentration points (≤ 5 pptv) are from CLOUD4 and are correct. The correction of the high concentration points from CLOUD7 therefore relates to data where nucleation rates were saturated with respect to DMA, and therefore the change does not affect any of the conclusions. Similarly, Kürten et al. (2014) reported DMA mixing ratios between 5 and 32 pptv during measurements of neutral sulfuric acid–DMA clusters. Applying the correction factor these values increase correspondingly. Since the exact DMA mixing ratios were not used in the data analysis by Kürten et al. (2014) the adjustment of the reported DMA values does not imply a significant change of the conclusions of Kürten et al. (2014).

3.5 Applicability to atmospheric measurements

Detection of amines by means of nitrate chemical ionization has the benefit that other substances relevant for new particle formation, such as sulfuric acid and ELVOCs, can be measured simultaneously with the same instrument. This is demonstrated in Fig. 7 for sulfuric acid concentrations up to 1.5×10^7 molecule $\mathrm{cm^{-3}}$ and DMA at 46 ± 12 pptv (i.e., 1.15×10^9 molecule $\mathrm{cm^{-3}}$), which shows that both compounds can be measured at the same time (data from

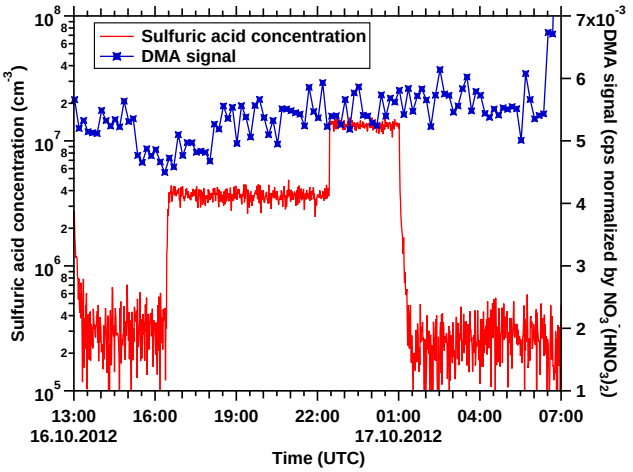

Figure 7. The time series of the normalized DMA signal and the $[H_2SO_4]$ are shown for a typical CLOUD7 run. The figure demonstrates that the DMA signal does not change significantly when H_2SO_4 is added even when the $[H_2SO_4]$ reaches $\sim 1.5 \times 10^7$ molecule cm^{-3}. The DMA mixing ratio shown here is 46 ± 12 pptv, which was measured by the IC instrument.

CLOUD7) and that the DMA signal is not affected by the presence of H_2SO_4 in this example. In situations where the DMA concentration is similar or lower than the sulfuric acid concentration, not all DMA molecules might, however, be detected due to clustering between sulfuric acid and DMA (see discussion further below). Figure 7 only shows the normalized DMA signals and no DMA mixing ratios because during the early phase of CLOUD7 the CI-APi-TOF was tuned differently and therefore the calibration curves from Fig. 5 could not be applied. In conclusion, it is crucial to calibrate the instrument for each instrumental setting.

Jen et al. (2015) have also performed measurements using nitrate chemical ionization while sulfuric acid and DMA were simultaneously present in a flow tube. However, they did not report signals at m/z 170 and m/z 233 Th, indicating that the nitrate DMA clusters were not present. We have no definitive explanation why Jen et al. (2015) could not observe these clusters but it might be related to the fact that they used rather high sulfuric acid concentrations (4×10^9 molecule cm^{-3}, i.e., ~ 160 pptv). DMA was also present at a relatively high mixing ratio (110 pptv); however the ratio between DMA and sulfuric acid was only about 0.7. From the paper by Jen et al. (2015) it is not evident whether the DMA mixing ratio was measured during the presence of sulfuric acid or before sulfuric acid was added. Assuming that the reported DMA mixing ratio was determined without sulfuric acid would probably mean that the actual DMA (free DMA molecules not bound to any other molecule or cluster) during the experiment with added sulfuric acid could be significantly lower because sulfuric acid monomers and clusters of sulfuric acid would efficiently deplete DMA at such a low DMA to sulfuric acid ratio (Ortega et al., 2012; Jen et al., 2014; Kürten et al., 2014). In the case that the DMA molecules are not "free" but attached to sulfuric acid (or to sulfuric acid clusters), they might not lead to a signal for $NO_3^- \cdot (HNO_3)_{1,2} \cdot$ (DMA) but rather end up in a cluster involving the bisulfate ion associated with sulfuric acid and DMA. Such mixed clusters (bisulfate, sulfuric acid, and DMA) were detected by Jen et al. (2015). In summary, the depletion of DMA by sulfuric acid and clusters could be responsible for the missing signals at m/z 170 and m/z 233 Th. If this was the case nitrate chemical ionization would yield accurate results for DMA measurements as it would only measure the free (unbound) portion of the amines and not the amine molecules clustered to sulfuric acid.

In terms of measuring the total amine concentration, the technique presented here will instead provide a lower limit when the sulfuric acid to amine ratio is on the order of 1 or larger. However, the same applies to the measurement of total sulfuric acid, which will also be higher than the sulfuric acid monomer concentration when several pptv of DMA are present because a significant fraction of sulfuric acid monomers can be incorporated in clusters (Rondo et al., 2016).

4 Conclusions

It is demonstrated that DMA can be detected at mixing ratios in the pptv range using nitrate chemical ionization mass spectrometry. DMA is mainly detected in a cluster containing the nitrate ion plus additional nitric acid molecules ($NO_3^- \cdot (HNO_3)_{1-3} \cdot$ (DMA)). Calibration of the CI-APi-TOF used during the CLOUD7 and CLOUD10-T campaign indicates very good linearity in the range between 0 and ~ 120 pptv of DMA. The detection limit under ideal conditions at the CLOUD chamber was below 1 pptv for an integration time of 10 min at a temperature of 278 K and a relative humidity of 38 %. While there are other techniques yielding similar or even better detection limits for DMA (or amine measurements in general) the method introduced in this study should allow for simultaneous measurements of sulfuric acid and ELVOCs. Both compounds are thought to play an essential role in the formation of new particles. Being capable of measuring DMA together with sulfuric acid and ELVOCs makes nitrate CI an even more versatile tool for studying new particle formation than previously thought.

Future studies will focus on the effect of temperature and RH regarding the sensitivity of nitrate CI towards DMA. Furthermore, the detection of other amines will be tested and the method will be deployed in field studies. For such measurements an amine calibration source providing well-defined concentrations to the CI-APi-TOF (e.g., Freshour et al., 2014) would be desirable.

Acknowledgements. We thank CERN for supporting CLOUD with important technical and financial resources and provision of a particle beam from the proton synchrotron. This research received funding from the EC Seventh Framework Programme (Marie Curie Initial Training Network MC-ITN "CLOUD-TRAIN" no. 316662), the German Federal Ministry of Education and Research (project no. 01LK1222A) as well as the Swiss National Science Foundation (project no. 200020_152907). We thank the tofTools team for providing tools for mass spectrometry analysis.

Edited by: J. Abbatt

References

Almeida, J., Schobesberger, S., Kürten, A., Ortega, I. K., Kupiainen-Määttä, O., Praplan, A. P., Adamov, A., Amorim, A., Bianchi, F., Breitenlechner, M., David, A., Dommen, J., Donahue, N. M., Downard, A., Dunne, E. M., Duplissy, J., Ehrhart, S., Flagan, R. C., Franchin, A., Guida, R., Hakala, J., Hansel, A., Heinritzi, M., Henschel, H., Jokinen, T., Junninen, H., Kajos, M., Kangasluoma, J., Keskinen, H., Kupc, A., Kurtén, T., Kvashin, A. N., Laaksonen, A., Lehtipalo, K., Leiminger, M., Leppä, J., Loukonen, V., Makhmutov, V., Mathot, S., McGrath, M. J., Nieminen, T., Olenius, T., Onnela, A., Petäjä, T., Riccobono, F., Riipinen, I., Rissanen, M., Rondo, L., Ruuskanen, T., Santos, F. D., Sarnela, N., Schallhart, S., Schnitzhofer, R., Seinfeld, J. H., Simon, M., Sipilä, M., Stozhkov, Y., Stratmann, F., Tomé, A., Tröstl, J., Tsagkogeorgas, G., Vaattovaara, P., Viisanen, Y., Virtanen, A., Vrtala, A., Wagner, P. E., Weingartner, E., Wex, H., Williamson, C., Wimmer, D., Ye, P., Yli-Juuti, T., Carslaw, K. S., Kulmala, M., Curtius, J., Baltensperger, U., Worsnop, D. R., Vehkamäki, H., and Kirkby, J.: Molecular understanding of sulphuric acid-amine particle nucleation in the atmosphere, Nature, 502, 359–363, 2013.

Berndt, T., Stratmann, F., Sipilä, M., Vanhanen, J., Petäjä, T., Mikkilä, J., Grüner, A., Spindler, G., Lee Mauldin III, R., Curtius, J., Kulmala, M., and Heintzenberg, J.: Laboratory study on new particle formation from the reaction $OH + SO_2$: influence of experimental conditions, H_2O vapour, NH_3 and the amine tert-butylamine on the overall process, Atmos. Chem. Phys., 10, 7101–7116, doi:10.5194/acp-10-7101-2010, 2010.

Berndt, T., Sipilä, M., Stratmann, F., Petäjä, T., Vanhanen, J., Mikkilä, J., Patokoski, J., Taipale, R., Mauldin III, R. L., and Kulmala, M.: Enhancement of atmospheric H_2SO_4 / H_2O nucleation: organic oxidation products versus amines, Atmos. Chem. Phys., 14, 751–764, doi:10.5194/acp-14-751-2014, 2014.

Bianchi, F., Praplan, A. P., Sarnela, N., Dommen, J., Kürten, A., Ortega, I. K., Schobesberger, S., Junninen, H., Simon, M., Tröstl, J., Jokinen, T., Sipilä, M., Adamov, A., Amorim, A., Almeida, J., Breitenlechner, M., Duplissy, J., Ehrhart, S., Flagan, R. C., Franchin, A., Hakala, J., Hansel, A., Heinritzi, M., Kangasluoma, J., Keskinen, H., Kim, J., Kirkby, J., Laaksonen, A., Lawler, M. J., Lehtipalo, K., Leiminger, M., Makhmutov, V., Mathot, S., Onnela, A., Petäjä, T., Riccobono, F., Rissanen, M. P., Rondo, L., Tomé, A., Virtanen, A., Viisanen, Y., Williamson, C., Wimmer, D., Winkler, P. M., Ye, P., Curtius, J., Kulmala, M., Worsnop, D. R., Donahue, N. M., and Baltensperger, U.: Insight into Acid–Base Nucleation Experiments by Comparison of the Chemical Composition of Positive, Negative, and Neutral Clusters, Environ. Sci. Technol., 48, 13675–13684, doi:10.1021/es502380b, 2014.

Chen, M., Titcombe, M., Jiang, J., Jen, C., Kuang, C., Fischer, M. L., Eisele, F. L., Siepmann, J. I., Hanson, D. R., Zhao, J., and McMurry, P. H.: Acid–base chemical reaction model for nucleation rates in the polluted atmospheric boundary layer, Proc. Natl. Acad. Sci. USA, 109, doi/10.1073/pnas.1210285109, 18713–18718, 2012.

Creamean, J. M., Ault, A. P., Ten Hoeve, J. E., Jacobson, M. Z., Roberts, G. C., and Prather, K. A.: Measurements of aerosol chemistry during new particle formation events at a remote rural mountain site, Environ. Sci. Technol., 45, 8208–8216, doi:10.1021/es103692f, 2011.

Crump, J. G. and Seinfeld, J. H.: Turbulent deposition and gravitational sedimentation of an aerosol in a vessel of arbitrary shape, J. Aerosol Sci., 12, 405–415, 1981.

Ehn, M., Thornton, J. A., Kleist, E., Sipilä, M., Junninen, H., Pullinen, I., Springer, M., Rubach, F., Tillmann, R., Lee, B., Lopez-Hilfiker, F., Andres, S., Acir, I.-H., Rissanen, M., Jokinen, T., Schobesberger, S., Kangasluoma, J., Kontkanen, J., Nieminen, T., Kurtén, T., Nielsen, L. B., Jørgensen, S., Kjaergaard, H. G., Canagaratna, M., Dal Maso, M., Berndt, T., Petäjä, T., Wahner, A., Kerminen, V.-M., Kulmala, M., Worsnop, D. R., Wildt, J., and Mentel, T. F.: A large source of low–volatility secondary organic aerosol, Nature, 506, 476–479, 2014.

Eisele, F. L. and Tanner, D. J.: Measurement of the gas phase concentration of H_2SO_4 and methane sulfonic acid and estimates of H_2SO_4 production and loss in the atmosphere, J. Geophys. Res., 98, 9001–9010, 1993.

Erupe, M. E., Viggiano, A. A., and Lee, S.-H.: The effect of trimethylamine on atmospheric nucleation involving H2SO4, Atmos. Chem. Phys., 11, 4767–4775, doi:10.5194/acp-11-4767-2011, 2011.

Freshour, N. A., Carlson, K. K., Melka, Y. A., Hinz, S., Panta, B., and Hanson, D. R.: Amine permeation sources characterized with acid neutralization and sensitivities of an amine mass spectrometer, Atmos. Meas. Tech., 7, 3611–3621, doi:10.5194/amt-7-3611-2014, 2014.

Ge, X. L., Wexler, A. S., and Clegg, S. L.: Atmospheric amines – Part I. A review, Atmos. Environ., 45, 524–546, doi:10.1016/j.atmosenv.2010.10.012, 2011a.

Ge, X. L., Wexler, A. S., and Clegg, S. L.: Atmospheric amines - Part II. Thermodynamic properties and gas/particle partitioning, Atmos. Environ., 45, 561–577, doi:10.1016/j.atmosenv.2010.10.013, 2011b.

Glasoe, W. A., Volz, K., Panta, B., Freshour, N., Bachman, R., Hanson, D. R., McMurry, P. H., and Jen, C.: Sulfuric acid nucleation: An experimental study of the effect of seven bases, J. Geophys. Res.-Atmos., 120, 1933–1950, doi:10.1002/2014JD022730, 2015.

Hanson, D. R. and Eisele, F.: Diffusion of H_2SO_4 in humidified nitrogen: Hydrated H_2SO_4, J. Phys. Chem. A, 104, 1715–1719, 2000.

Hanson, D. R., McMurry, P. H., Jiang, J., Tanner, D., and Huey, L. G.: Ambient pressure proton transfer mass spectrometry: Detection of amines and ammonia, Environ. Sci. Technol., 45, 8881–8888, doi:10.1021/es201819a, 2011.

Jen, C. N., McMurry, P. H., and Hanson, D. R.: Stabilization of sulfuric acid dimers by ammonia, methylamine, dimethylamine, and trimethylamine, J. Geophys. Res.-Atmos., 119, 7502–7514, 10.1002/2014JD021592, 2014.

Jen, C. N., Hanson, D. R., and McMurry, P. H.: Towards Reconciling Measurements of Atmospherically Relevant Clusters by Chemical Ionization Mass Spectrometry and Mobility Classification/Vapor Condensation, Aerosol Sci. Tech., ARL, 49, i–iii, doi:10.1080/02786826.2014.1002602, 2015.

Jokinen, T., Sipilä, M., Junninen, H., Ehn, M., Lönn, G., Hakala, J., Petäjä, T., Mauldin III, R. L., Kulmala, M., and Worsnop, D. R.: Atmospheric sulphuric acid and neutral cluster measurements using CI-APi-TOF, Atmos. Chem. Phys., 12, 4117–4125, doi:10.5194/acp-12-4117-2012, 2012.

Junninen, H., Ehn, M., Petäjä, T., Luosujärvi, L., Kotiaho, T., Kostiainen, R., Rohner, U., Gonin, M., Fuhrer, K., Kulmala, M., and Worsnop, D. R.: A high-resolution mass spectrometer to measure atmospheric ion composition, Atmos. Meas. Tech., 3, 1039–1053, doi:10.5194/amt-3-1039-2010, 2010.

Karlsson, M. N. A. and Martinsson, B. G.: Methods to measure and predict the transfer function size dependence of individual DMAs, J. Aerosol Sci., 34, 603–625, 2003.

Kirkby, J., Curtius, J., Almeida, J., Dunne, E., Duplissy, J., Ehrhart, S., Franchin, A., Gagné, S., Ickes, L., Kürten, A., Kupc, A., Metzger, A., Riccobono, F., Rondo, L., Schobesberger, S., Tsagkogeorgas, G., Wimmer, D., Amorim, A., Bianchi, F., Breitenlechner, M., David, A., Dommen, J., Downard, A., Ehn, M., Flagan, R.C., Haider, S., Hansel, A., Hauser, D., Jud, W., Junninen, H., Kreissl, F., Kvashin, A., Laaksonen, A., Lehtipalo, K., Lima, J., Lovejoy, E. R., Makhmutov, V., Mathot, S., Mikkilä, J., Minginette, P., Mogo, S., Nieminen, T., Onnela, A., Pereira, P., Petäjä, T., Schnitzhofer, R., Seinfeld, J. H., Sipilä, M., Stozhkov, Y., Stratmann, F., Tomé, A., Vanhanen, J., Viisanen, Y., Vrtala, A., Wagner, P. E., Walther, H., Weingartner, E., Wex, H., Winkler, P. M., Carslaw, K. S., Worsnop, D. R., Baltensperger, U., and Kulmala, M.: Role of sulphuric acid, ammonia and galactic cosmic rays in atmospheric aerosol nucleation, Nature, 476, 429–435, 2011.

Kupc, A., Amorim, A., Curtius, J., Danielczok, A., Duplissy, J., Ehrhart, S., Walther, H., Ickes, L., Kirkby, J., Kurten, A., Lima, J. M., Mathot, S., Minginette, P., Onnela, A., Rondo, L., and Wagner, P. E.: A fibre-optic UV system for H_2SO_4 production in aerosol chambers causing minimal thermal effects, J. Aerosol Sci., 42, 532–543, doi:10.1016/j.jaerosci.2011.05.001, 2011.

Kürten, A., Rondo, L., Ehrhart, S., and Curtius, J.: Performance of a corona ion source for measurement of sulfuric acid by chemical ionization mass spectrometry, Atmos. Meas. Tech., 4, 437–443, doi:10.5194/amt-4-437-2011, 2011.

Kürten, A., Rondo, L., Ehrhart, S., and Curtius, J.: Calibration of a chemical ionization mass spectrometer for the measurement of gaseous sulfuric acid, J. Phys. Chem. A, 116, 6375–6386, doi:10.1021/jp212123n, 2012.

Kürten, A., Jokinen, T., Simon, M., Sipilä, M., Sarnela, N., Junninen, H., Adamov, A., Almeida, J., Amorim, A., Bianchi, F., Breitenlechner, M., Dommen, J., Donahue, N. M., Duplissy, J., Ehrhart, S., Flagan, R. C., Franchin, A., Hakala, J., Hansel, A., Heinritzi, M., Hutterli, M., Kangasluoma, J., Kirkby, J., Laaksonen, A., Lehtipalo, K., Leiminger, M., Makhmutov, V., Mathot, S., Onnela, A., Petäjä, T., Praplan, A. P., Riccobono, F., Rissanen, M. P., Rondo, L., Schobesberger, S., Seinfeld, J. H., Steiner, G., Tomé, A., Tröstl, J., Winkler, P. M., Williamson, C., Wimmer, D., Ye, P., Baltensperger, U., Carslaw, K. S., Kulmala, M., Worsnop, D. R., and Curtius, J.: Neutral molecular cluster formation of sulfuric acid-dimethylamine observed in real-time under atmospheric conditions, Proc. Natl. Acad. Sci. USA, 111, 15019–15024, doi:10.1073/pnas.1404853111, 2014.

Kurtén, T., Loukonen, V., Vehkamäki, H., and Kulmala, M.: Amines are likely to enhance neutral and ion-induced sulfuric acid-water nucleation in the atmosphere more effectively than ammonia, Atmos. Chem. Phys., 8, 4095–4103, doi:10.5194/acp-8-4095-2008, 2008.

Mäkelä, J., Yli-Koivisto, S., Hiltunen, V., Seidl, W., Swietlicki, E., Teinilä, K., Sillanpää, M., Koponen, I., Paatero, J., Rosman, K., and Hämeri, K.: Chemical composition of aerosol during particle formation events in boreal forest, Tellus B, 53, 380–393, doi:10.1034/j.1600-0889.2001.530405.x, 2001.

Luts, A., Parts, T.-E., Hõrrak, U., Junninen, H., and Kulmala, M.: Composition of negative air ions as a function of ion age and selected trace gases: Mass- and mobility distribution, J. Aerosol Sci., 42, 820–838, 2011.

Ortega, I. K., Kupiainen, O., Kurtén, T., Olenius, T., Wilkman, O., McGrath, M. J., Loukonen, V., and Vehkamäki, H.: From quantum chemical formation free energies to evaporation rates, Atmos. Chem. Phys., 12, 225–235, doi:10.5194/acp-12-225-2012, 2012.

Ortega, I. K., Olenius, T., Kupiainen-Määttä, O., Loukonen, V., Kurtén, T., and Vehkamäki, H.: Electrical charging changes the composition of sulfuric acid-ammonia/dimethylamine clusters, Atmos. Chem. Phys., 14, 7995–8007, doi:10.5194/acp-14-7995-2014, 2014.

Praplan, A. P., Bianchi, F., Dommen, J., and Baltensperger, U.: Dimethylamine and ammonia measurements with ion chromatography during the CLOUD4 campaign, Atmos. Meas. Tech., 5, 2161–2167, doi:10.5194/amt-5-2161-2012, 2012.

Rao, N. and McMurry, P. H.: Nucleation and Growth of Aerosol in Chemically Reacting Systems, Aerosol Sci. Technol., 11, 120–132, 1989.

Rondo, L., Ehrhart, S., Kürten, A., Adamov, A., Bianchi, F., Breitenlechner, M., Duplissy, J., Franchin, A., Dommen, J., Donahue, N. M., Dunne, E.M., Flagan, R. C., Hakala, J., Hansel, A., Keskinen, H., Kim, J., Jokinen, T., Lehtipalo, K., Leiminger, M., Praplan, A., Riccobono, F., Rissanen, M. P., Sarnela, N., Schobesberger, S., Simon, M., Sipilä, M., Smith, J. N., Tomé, A., Tröstl, J., Tsagkogeorgas, G., Vaattovaara, P., Winkler, P. M., Williamson, C., Wimmer, D., Baltensperger, U., Kirkby, J., Kulmala, M., Petäjä, T., Worsnop, D. R., and Curtius, J.: Effect of dimethylamine on the gas phase sulfuric acid concentration measured by Chemical Ionization Mass Spectrometry, J. Geophys. Res. Atmos., 121, 3036–3049, doi:10.1002/2015JD023868, 2016.

Sipilä, M., Sarnela, N., Jokinen, T., Junninen, H., Hakala, J., Rissanen, M. P., Praplan, A., Simon, M., Kürten, A., Bianchi, F., Dommen, J., Curtius, J., Petäjä, T., and Worsnop, D. R.: Bisulfate – cluster based atmospheric pressure chemical ionization mass spectrometer for high-sensitivity (< 100 ppqV) detection of atmospheric dimethyl amine: proof-of-concept and first ambient data from boreal forest, Atmos. Meas. Tech., 8, 4001-4011, doi:10.5194/amt-8-4001-2015, 2015.

Smith, J. N., Barsanti, K. C., Friedli, H. R., Ehn, M., Kulmala, M., Collins, D. R., Scheckman, J. H., Williams, B. J., and McMurry, P. H.: Observations of aminium salts in atmospheric nanoparticles and possible climatic implications, P. Natl. Acad. Sci. USA, 107, 6634–6639, doi:10.1073/pnas.0912127107, 2010.

Tanner, D. J. and Eisele, F. L.: Ions in oceanic and continental air masses, J. Geophys. Res., 96, 1023–1031, doi:10.1029/90JD02131, 1991.

Voigtländer, J., Duplissy, J., Rondo, L., Kürten, A., and Stratmann, F.: Numerical simulations of mixing conditions and aerosol dynamics in the CERN CLOUD chamber, Atmos. Chem. Phys., 12, 2205–2214, doi:10.5194/acp-12-2205-2012, 2012.

Yu, H. and Lee, S. H.: Chemical ionisation mass spectrometry for the measurement of atmospheric amines, Environ. Chem., 9, 190–201, doi:10.1071/EN12020, 2012.

Zhao, J., Smith, J. N., Eisele, F. L., Chen, M., Kuang, C., and McMurry, P. H.: Observation of neutral sulfuric acid-amine containing clusters in laboratory and ambient measurements, Atmos. Chem. Phys., 11, 10823–10836, doi:10.5194/acp-11-10823-2011, 2011.

Zollner, J. H., Glasoe, W. A., Panta, B., Carlson, K. K., McMurry, P. H., and Hanson, D. R.: Sulfuric acid nucleation: power dependencies, variation with relative humidity, and effect of bases, Atmos. Chem. Phys., 12, 4399–4411, doi:10.5194/acp-12-4399-2012, 2012.